Fault-tolerant and Reconfigurable Control of Unmanned Aerial Vehicles (UAVs)

Final Technical Report

Yong D. Song

Professor
Department of Electrical and Computer Engineering
North Carolina A&T State University, Greensboro, NC 27411

February 29, 2008

Summary

Unmanned aerial vehicles (UAVs) are critical components of the future naval forces. UAV control and monitoring with autonomous operation will become an absolute necessity and adaptive cooperation of vehicles is the only practical alternative.

The objective of this project is to develop and evaluate new methodologies for cooperative (formation) control of multiple unmanned air vehicles. The goal is to have multiple UAVs working together as a group. Instead of separately assigning distinct tasks to each vehicle, the operator would assign tasks to the UAV group, which then determines the best way to accomplish each task, freeing the operator to maintain surveillance over the entire operation. In this project we investigated Path Tracking and obstacle avoidance of UAVs using fuzzy logic method. Algorithms for close formation control of multi-UAVs are developed and simulated. We also investigated fault-tolerant control of single UAVs by neuro-adaptive method. Detailed description of this method is provided in this document. The project has supported 5 graduate students with 9 technical papers published.

Technical Details

A. Path Tracking and Obstacle Avoidance of UAVs

Unmanned Aerial Vehicles (UAVs) have attracted increasing attention in the military and civilian applications, such as mapping, patrolling, search and rescue, and reconnaissance. In these types of applications, the Path tracking and Obstacle avoidance are fundamental. In this work, we developed a fuzzy logic based approach to path tracking and obstacle avoiding. We consider the case that obstacles are either still or moving and appear along the pre-determined flight path unexpectedly. By using suitable sensors we identify the relative distance between the vehicle and the obstacle and make timely adjustment to the pre-planned flight path. Fuzzy logic control algorithms are developed to achieve close path tracking while avoiding obstacles. Some simulation results are presented in Figure 1-Figure 6.

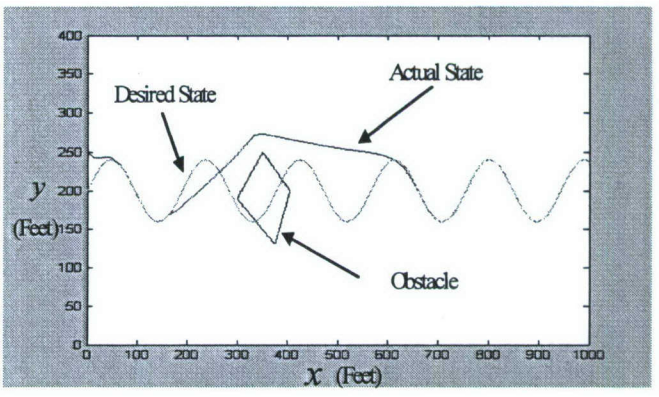

Figure 1 - Path tracking with one obstacle – shape 1

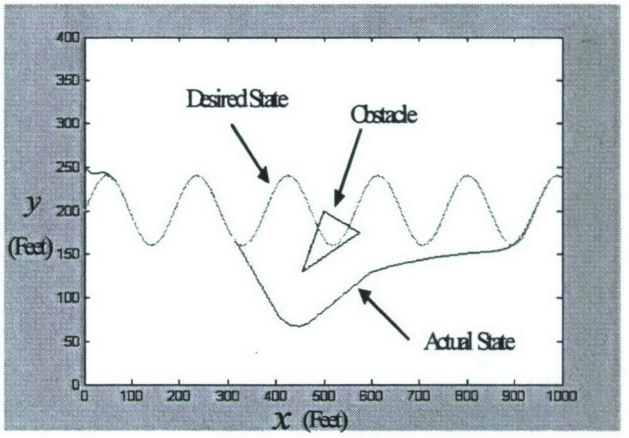

Figure 2 - Path tracking with one obstacle- shape 2

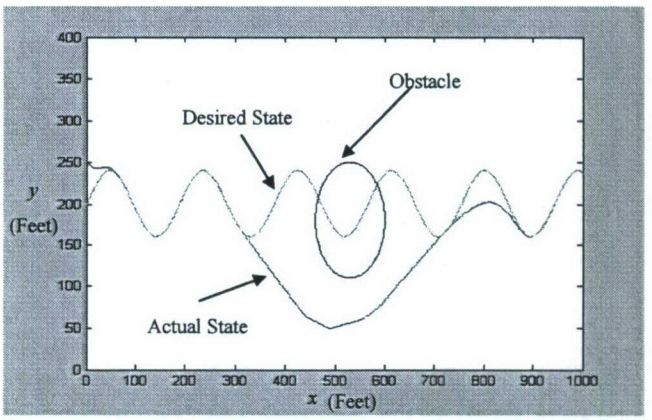

Figure 3 - Path tracking with one obstacle- shape 3

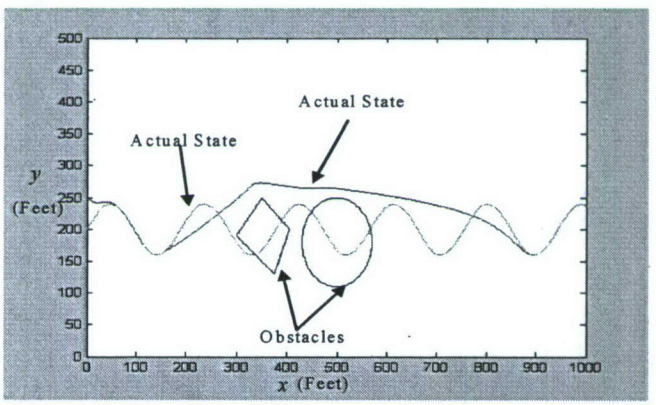

Figure 4 - Path tracking with two obstacles along the same Line

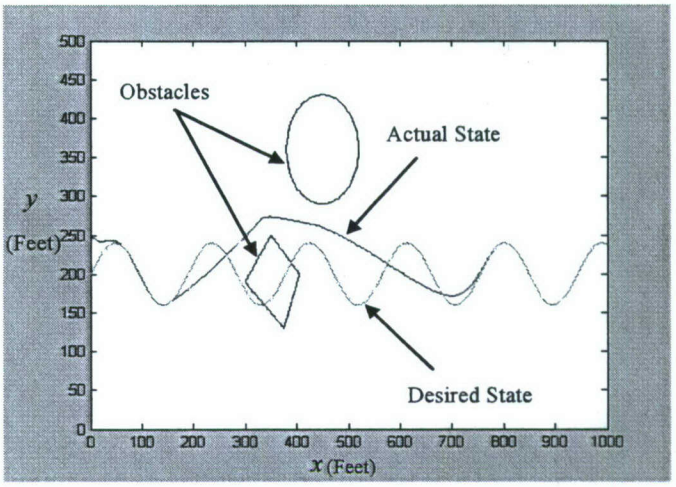

Figure 5 - Path tracking with two obstacles across the flight path

B. Fuzzy Logic based Control of multi-UAVs

We also explored a method to achieve close formation tracking control of multi-UAVs by applying fuzzy logic theory. The formation trajectory is achieved by the control of Wingman's heading velocity and heading angle while the lead UAV is maneuvering the given mission path. Since the values for specifying linguistic terms of the controller output for trailing UAV actually determine the shape of the input-output shape, they are selected as the main parameters for optimization. We have successfully used such a fuzzy controller to approximate the nonlinear system, which can be applied for the supervised learning.

The method guarantees the desired tracking precision and also ensures the control action smooth under system uncertainties and external disturbances. Simulation of leader-wingman formation geometry was conducted. Both theoretical studies and simulation results demonstrate that this control algorithm is simple, less sensitive to the flight aerodynamic model. The formation geometry is determined by the relative position between the Leader and Wingman as shown in Figure 6. The formation control objective is to steer the Wingman (follower) to maintain certain separation distance in longitudinal, lateral and vertical directions.

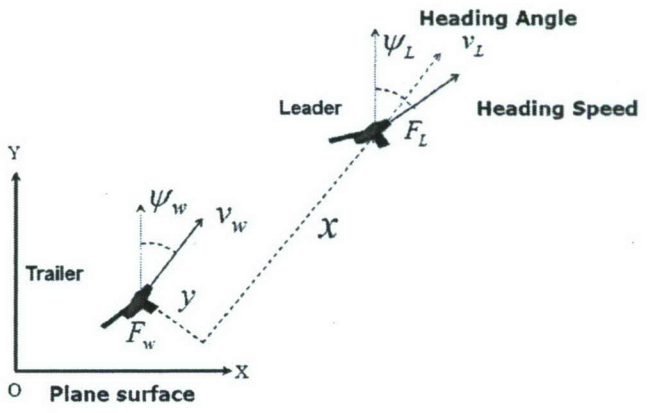

Figure 6 - Formation flight in inertial frame

Table 1: Parameters Used for Simulation

Wing Area	300	ft2
Wing Span	30	ft
Mass	776.4	lb
Altitude	45,000	ft
Dynamic Pressure	155.8	lb/ft2
Mach	0.85	mach
$[x,\ y,\ z]$	$\begin{bmatrix} 100\text{ft} & 60\text{ft} & 0\text{ft} \\ 90\text{ft} & -50\text{ft} & 0\text{ft} \end{bmatrix}$	
$[x_d, y_d, z_d]$	$\begin{bmatrix} 60\text{ft} & 30\pi/4\text{ft} & 0\text{ft} \\ 60\text{ft} & -30\pi/4\text{ft} & 0\text{ft} \end{bmatrix}$	
$[V_w(0),\ \psi_w(0),\ h_w(0)]$	[750ft/s, $\pi/6$, 30,000ft]	
$[V_L,\ \psi_L,\ h_L]$	[825ft/s, $\pi/8$, 30,000ft]	

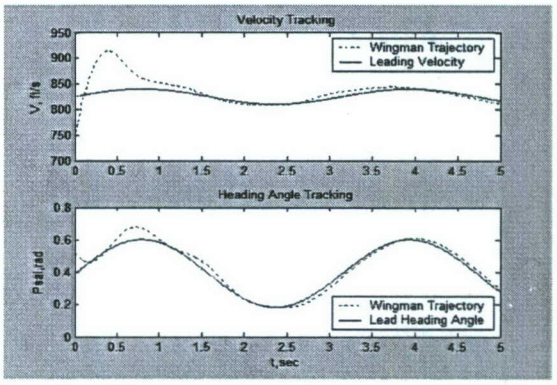

Figure 7a - Tracking trajectory of a sinusoid function

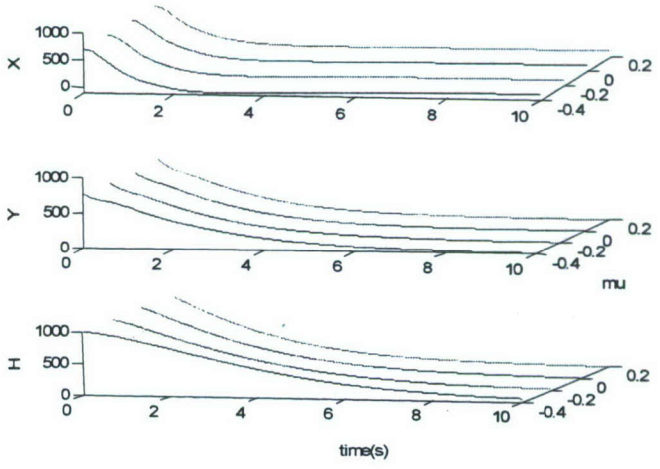

Figure 7b - Separation tracking errors of wingman A

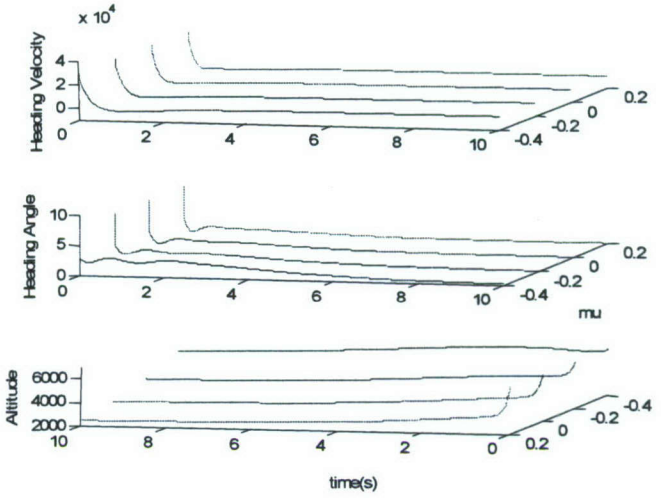

Figure 7c - Separation control signals of wingman A

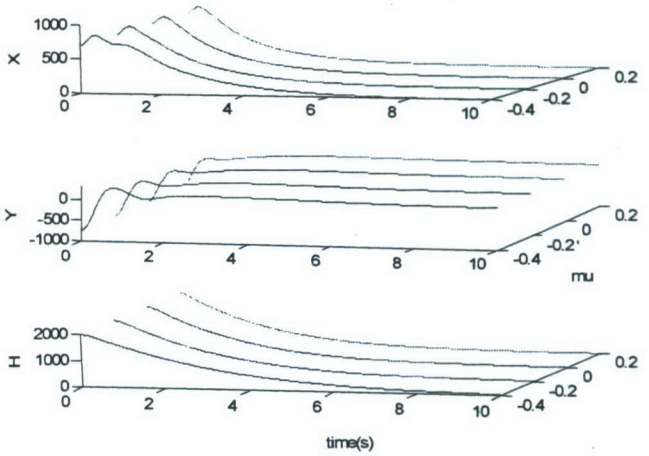

Figure 7d - Separation tracking errors of wingman B

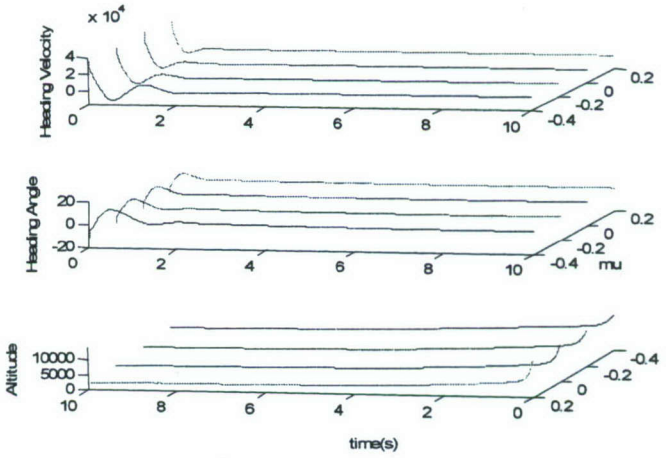

Figure 7e - Separation control signals of wingman B

Neuro-robust and adaptive control algorithms and memory-based control algorithms for close formation control have been developed. A series of simulations have been carried out. Some of the results based on the parameters and conditions as in Table 1 are presented in Figure 7a-Figure 7e. As clearly indicated from the results, the proposed method maintains a desired tracking precision and also ensures the control action smooth under the system uncertainties and external disturbances.

C. Neuro-adaptive based Fault-tolerant Control

One of the typical yet devastating faults in flight systems is the loss of the driving (propulsion) power. In this work, we explore an innovative approach to accommodate such faults in unmanned aerial vehicles operating under varying fight conditions.

We present a neuro-adaptive control strategy, composed of two Neural Network (NN) units, the former to adapt to unanticipated uncertainties and the latter to enhance performance by compensating (funneling) the estimation error caused by the first NN to incorporate the important and most common problem faced by the airborne vehicles, unforeseen and uncertain actuating failures. New algorithms are derived to cope with the sub-system failures due to the jet engine partially losing its propulsion power ensuring the system stability. Simulation study using a generic model demonstrates a dramatically improved performance in the face of fading power faults and system uncertainties. Some of the details are presented as follows.

C.1. Introduction

Every component in a flight vehicle provides a certain vital function and the overall system works satisfactorily only if all components provide the service they are designed for, accurately. Therefore, a fault in a single component usually degrades the performance of the overall flight. In order to avoid performance deteriorations or damage to the vehicle, faults have to be identified and accommodated in a timely manner. In UAV, failures of control elements (sensors, actuators, etc.) are often encountered. A weak element in this framework is control loops. In fact automated systems are vulnerable to faults such as defects in sensors or in actuators, which can cause undesired reactions and consequences. A conventional feedback control design for a complex system such as UAV may result in unsatisfactory performance, or instability or malfunctions in system components, causing serious operation and safety problems. Therefore, fault tolerance has been one of the major issues in control of flight vehicles.[1].

A closed-loop control system able to tolerate component malfunctions while maintaining desirable system performance and stability exhibits *fault-tolerant* property. These systems, also termed as self-repairing systems, have been a subject of widely scattered studies. In this framework, the design of Fault Tolerant Control architecture is of crucial importance and solutions aiming at adapting the control strategy to the presence of the fault are needed in order to achieve prescribed performances. This is usually achieved by providing the control loop with a decision making layer that analyzes the behavior of the plant and adapts the control strategy to hold the controlled system in a region of acceptable performances. This is also phrased as Fault Tolerant Control (FTC).

Fading power failure causes major problems in many critical control systems such as flight control systems. It is often not known when a jet propulsion fails and how much the failure is but

the remaining power could be still enough to accomplish a desired control task such as emergency landing of a flight vehicle. The question is whether a control system is intelligent enough to use remaining thrust in the presence of unknown failures. Figure 8 illustrates the general fault scenario. An adaptive approach, which is capable of controlling systems with uncertainties, is thus of interest in developing control schemes which are efficient for handling unknown sub-system failures.

Most existing fault-tolerant control systems are built with redundant controllers[2-4]. The backup control loop is employed once failure of the main controller is detected online. However, often times, the additional cost, space and complexity of incorporating redundant hardware makes this approach unattractive. The use of redundant controllers may significantly increase the capital and maintenance costs of such control systems to unacceptable levels. Therefore, fault-tolerant control systems with no or less control redundancy are desirable.

Redundancy free fault tolerant control has been studied recently. One approach is to detect and diagnose system faults online and update control laws accordingly to stabilize faulty system[1]. However this method is usually difficult to implement, as it required multiple control algorithms to be pre-programmed for each possible failure scenario. Various approaches to achieve control reconfiguration have been researched[5, 6-8]. Fault-tolerant control systems can benefit from blending the perspectives of intelligent control. Passino[9] describes some of the

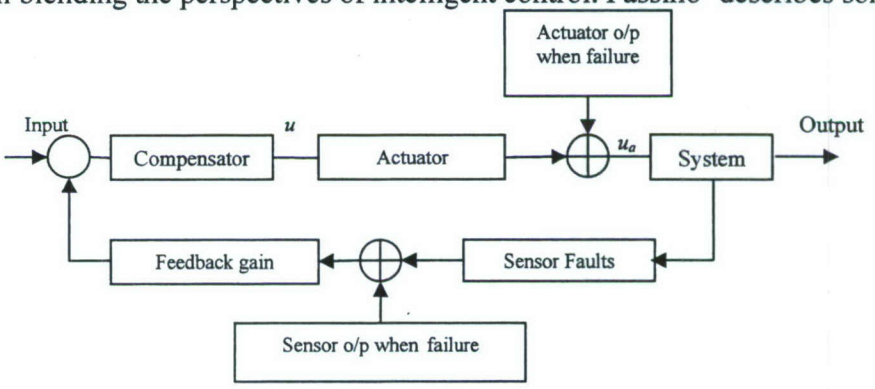

Figure 8 - The general fault scenario

limitations of current approaches, and states that a combination of intelligent and conventional control methods may be the best way to implement autonomous control. However, from the application point of view, only a few studies have been devoted to flight vehicles. Rauch[10] talks about fault accommodation in flight and space shuttle control, where Probabilistic Neural Networks are used. Polycarpou et al.[11] presented a neural network (NN) based fault tolerant approach and application on Beaver aircraft but did not mention fault occurrence in the primary flight control system. Chen et al.[12] presented an LMI-based synthesis scheme for robust fault-tolerant control systems design, where an unmanned aircraft suffering from wing impairment is used as a design example. Boskovik et al.[13] presented a new Decentralized Failure Detection and Identification (FDI) and Adaptive Reconfigurable Control (ARC) scheme, well suited for achieving the desired flight performance in the presence of multiple and applications to F-18 aircraft carrier landing maneuver. NN model based FTC has been studied in recent years[14]. However, the key point of applying NNs to the FTC of a practical system is that this model must

be able to approximate the system faults with sufficient accuracy and satisfy the real time requirement.

Our objective is to design a fault tolerant flight control system guaranteeing stability and satisfactory performance not only when all components are operational, but also in the case when actuating power fades and failures occur in flight dynamics. We propose a neuro-adaptive control scheme that is capable of tolerating component malfunctions and fading jet-engine power, while still maintaining desirable performance and stability properties. It possesses loop integrity, reliability, maintainability and survivability. The NN used in this work is an online-trained network in which the weights are adjusted online accordingly to accommodate faults occurring during system operation.

C.2. Flight Vehicles Dynamics with Faults

FTC systems can be characterized as robust, reconfigurable or a combination of both. The flight vehicles, regardless whether they are military or commercial, require precise maneuverability and control; therefore, the design of a robust controller that assures a safe and precise operation of the flight vehicle is of extreme importance. A great difficulty related with the design of any flight control system is that a complete and accurate dynamic model – including aerodynamic coefficients, is required. However, it is difficult to identify accurately the aerodynamic coefficients because they are nonlinear functions of several physical variables. Neural networks have been proposed recently as an adaptive controller for nonlinear systems. The development and analysis of NN based control algorithms for the control planes of flight vehicles with faulty dynamics, varying mass, nonlinear velocity and parameter uncertainties is a very challenging task.

The trajectory tracking of a flight vehicle is achieved through the help of control planes, which in turn are adjusting the angles of attack, sideslip and body-axis roll of the flight vehicle. These angles can be observed in Figure 9. We use the dynamics similar to X-37 represent the nonlinear mathematical model of flight vehicles. The controllers are designed with the assumption that some of the aerodynamic coefficients are fully understood.

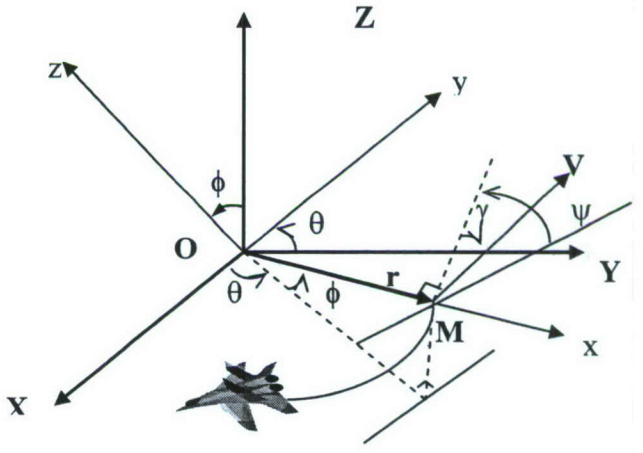

Figure 9 - Coordinate System

The body-fixed axes, nonlinear equation of motion for a UAV over a flat Earth are given by Lee and that describes a similar model as follows[15, 16]:

$$\dot{V} = \frac{\cos\alpha\cos\beta}{m}\left[T + F_x\right] + \frac{\sin\beta}{m}\left[F_y\right] + \frac{\sin\alpha\cos\beta}{m}\left[F_z\right] + g\left[-\cos\alpha\cos\beta\sin\theta + \sin\beta\sin\phi\cos\theta + \sin\alpha\cos\beta\cos\phi\cos\theta\right] \tag{1}$$

$$\dot{\alpha} = -\cos\alpha\tan\beta p + q - \sin\alpha\tan\beta r - \frac{\sin\alpha}{mV\cos\beta}\left[T + F_x\right] + \frac{\cos\alpha}{mV\cos\beta}F_z + \frac{g}{V\cos\beta}\left[\sin\alpha\sin\theta + \cos\alpha\cos\phi\cos\theta\right] \tag{2}$$

$$\dot{\beta} = \sin\alpha p - \cos\alpha r - \frac{\sin\alpha\sin\beta}{mV}\left[T + F_x\right] + \frac{\cos\beta}{mV}F_y - \frac{\sin\alpha\sin\beta}{mV}F_z + \frac{g}{V}\left[\cos\alpha\sin\beta\sin\theta + \cos\beta\cos\theta\sin\phi - \sin\alpha\sin\beta\cos\phi\cos\theta\right] \tag{3}$$

$$\begin{aligned} \dot{p} &= I_2 pq + I_1 qr + I_3 L + I_4 N \\ \dot{q} &= I_5 pr - I_6\left(p^2 - r^2\right) + I_7 M \\ \dot{r} &= -I_2 qr + I_8 pq + I_4 L + I_9 N \end{aligned} \tag{4}$$

where the moments of inertia I_i, $i=1,2,\ldots 9$ are defined as follows:

$$\begin{aligned} I_1 &= -\frac{I_z\left(I_z - I_y\right) - I_{xz}^2}{I_x I_z - I_{xz}^2}, I_2 = \frac{I_{xz}I_x + \left(I_z - I_y\right)}{I_x I_z - I_{xz}^2}, I_3 = \frac{I_z}{I_x I_z - I_{xz}^2}, I_4 = \frac{I_{xz}}{I_x I_z - I_{xz}^2} \\ I_5 &= \frac{I_z - I_x}{I_y} I_6 = \frac{I_{xz}}{I_y}, I_7 = \frac{1}{I_y}, I_8 = \frac{I_x\left(I_x - I_y\right) + I_{xz}^2}{I_x I_z - I_{xz}^2}, I_9 = \frac{I_x}{I_x I_z - I_{xz}^2} \end{aligned} \tag{5}$$

Definition of state and control variables, forces and moments in the preceding equations are described in the Nomenclature. It is assumed that the aerodynamic forces and moments are expressed as functions of angle of attack, sideslip angle, angular rates, and control surface deflection. *L, M,* and *N* are expressed as follows[16]:

$$\begin{aligned} L &= \left[C_l(\alpha,\beta) + C_{l\delta a}(\alpha,\beta)\delta_a + C_{l\delta r}(\alpha,\beta)\delta_r + \frac{bp}{2V}C_{lp}(\alpha) + \frac{br}{2V}C_{lr}(\alpha)\right]\bar{q}Sb \\ M &= \left[C_m(\alpha,\beta) + C_{m\delta e}(\alpha,\beta)\delta_e + \frac{rb}{2V}C_{mr}(\alpha) + \frac{q\bar{c}}{V}C_{mq}(\alpha)\right]\bar{q}S\bar{c} \\ N &= \left[C_n(\alpha,\beta) + C_{n\delta a}(\alpha,\beta)\delta_a + C_{n\delta r}(\alpha,\beta)\delta_r + \frac{bp}{2V}C_{np}(\alpha)\frac{br}{2V}C_{nr}(\alpha)\frac{q\bar{c}}{V}C_{nq}(\alpha)\right]\bar{q}Sb \end{aligned} \tag{6}$$

The moments, coefficients and parameters are described in the Appendix. Substituting the aerodynamic coefficients into the flight dynamic equations yields the following:

$$\begin{bmatrix}\dot{\alpha}\\ \dot{\beta}\\ \dot{\phi}\end{bmatrix}=\begin{bmatrix}-\cos\alpha\tan\beta & 1 & -\sin\alpha\tan\beta\\ \sin\alpha & 0 & -\cos\alpha\\ 1 & \sin\phi\tan\theta & \cos\phi\tan\theta\end{bmatrix}\begin{bmatrix}p\\ q\\ r\end{bmatrix}$$
$$+\frac{g}{V}\begin{bmatrix}\frac{1}{\cos\beta}(\sin\alpha\sin\theta+\cos\alpha\cos\phi\cos\theta)\\ \cos\alpha\sin\beta\sin\theta+\cos\beta\cos\theta\sin\phi-\sin\alpha\sin\beta\cos\phi\cos\theta\\ 0\end{bmatrix}$$
$$+\begin{bmatrix}-\frac{\sin\alpha}{mV\cos\beta}[T+F_x]+\frac{\cos\alpha}{mV\cos\beta}F_z\\ \frac{-\sin\alpha\sin\beta}{mV}[T+F_x]+\frac{\cos\beta}{mV}F_y-\frac{-\sin\alpha\sin\beta}{mV}F_z\\ 0\end{bmatrix} \tag{7}$$

$$\begin{bmatrix}\dot{p}\\ \dot{q}\\ \dot{r}\end{bmatrix}=\begin{bmatrix}I_2pq+I_1qr\\ I_5pr-I_6\left(p^2-r^2\right)\\ -I_2qr+I_8pq\end{bmatrix}+\begin{bmatrix}I_3C_l(\alpha,\beta)\bar{q}Sb+I_4C_n(\alpha,\beta)\bar{q}Sb\\ I_7C_m(\alpha)\bar{q}S\bar{c}\\ I_4C_l(\alpha,\beta)\bar{q}Sb+I_9C_n(\alpha,\beta)\bar{q}Sb\end{bmatrix}$$
$$+\frac{\rho VS}{4}\begin{bmatrix}I_3C_{lp}(\alpha)b+I_4C_{np}(\alpha)b & 0 & I_3C_{lr}(\alpha)b+I_4C_{nr}(\alpha)b\\ 0 & I_7C_{mq}(\alpha)\bar{c} & 0\\ I_4C_{lp}(\alpha)b+I_9C_{np}(\alpha)b & 0 & I_4C_{lr}(\alpha)b+I_9C_{nr}(\alpha)b\end{bmatrix}\begin{bmatrix}p\\ q\\ r\end{bmatrix} \tag{8}$$
$$+\bar{q}S\begin{bmatrix}0 & I_3C_{l\delta_a}(\alpha,\beta)b+I_4C_{n\delta_a}(\alpha,\beta)b & I_3C_{l\delta_r}(\alpha,\beta)b+I_4C_{n\delta_r}(\alpha,\beta)b\\ I_7C_{m\delta_e}(\alpha)\bar{c} & 0 & 0\\ 0 & I_4C_{l\delta_a}(\alpha,\beta)b+I_9C_{n\delta_a}(\alpha,\beta)b & I_4C_{l\delta_r}(\alpha,\beta)b+I_9C_{n\delta_r}(\alpha,\beta)b\end{bmatrix}\begin{bmatrix}\delta_e\\ \delta_a\\ \delta_r\end{bmatrix}$$

$$\begin{bmatrix}\dot{\theta}\\ \dot{\psi}\end{bmatrix}=\begin{bmatrix}0 & \cos\phi & -\sin\phi\\ 0 & \frac{\sin\phi}{\cos\theta} & \frac{\cos\phi}{\cos\theta}\end{bmatrix}\begin{bmatrix}p\\ q\\ r\end{bmatrix} \tag{9}$$

Naming the states $x=[\alpha\ \ \beta\ \ \phi]^T$, $y=[p\ \ q\ \ r]^T$ and $z=[\theta\ \ \psi]^T$, the nonlinear dynamic system under consideration can be described as follows:

$$\dot{x}=A(\alpha,\beta,\phi,\theta)+B(\alpha,\beta,\phi,\theta)y(p,q,r) \tag{10}$$

$$\dot{y}=C(\alpha,\beta,p,q,r)+D(\alpha)y(p,q,r)+E(\alpha,\beta)u \tag{11}$$

$$\dot{z}=H(\phi,\theta)y(p,q,r) \tag{12}$$

where A, B, C, D, E and H represents the grouped terms of Eq. (10) – Eq. (12) in order and $u = [\delta_e \quad \delta_a \quad \delta_r]$ is the control input

Remark:

The mass m of the reusable vehicle is considered time-varying due to the m_f fuel consumption - especially during the ascend mode. Therefore, the total mass of the vehicle is:

$$m = m_0 + m_f + m_p$$

where

m_o real dry weight

m_f fuel weight (variable)

m_p payload weight

Note that this change in mass affects the dynamics, however, the change in UAV's mass dm/dt is considered unknown, making m unknown in the model, thus should not be used directly in control design.

Observations:

- The simulation studies show that the norm of the gain matrix from Eq. (10) is negligible, and therefore, this leads to a simplification of the dynamic model under consideration without any lost of generality.
- The dynamic system equation described in Eq. (10) – Eq. (12) is controllable only if the matrix BE is invertible. Matrix E is known from the literature as being invertible. As for matrix B, the control surfaces of the reusable launch vehicle are designed to control each axes angular rate of aircraft independently; therefore, the matrix B is invertible for all cases. Numerical studies for the aerodynamic model also show that B is always invertible. The dynamic system presented can be recast in the second-order form by deriving Eq. (8) and substituting Eq. (9); it can follow:

$$\ddot{x} = \frac{d}{dt}A(.) + BC + \left[\frac{d}{dt}B(.) + BD\right]y + BEu \tag{13}$$

The above equation is the governing equation of motion for the aircraft and will be used for the control design and stability analysis processes of the following sections. All the effects caused by possible failures in the system can be lumped into an uncertain term. The fault dynamics can be described as follows:

$$f_f = \pm\chi(t - T_f)\Gamma(.) \text{ with}$$
$$\chi(t - T_f) = \begin{cases} 0 & \text{if} \quad t < T_f \\ 1 - e^{\alpha_f (t - T_f)} & \text{otherwise} \end{cases} \tag{14}$$

Note that the faulty function described above covers both the jump and continuously time varying faults in both directions. The additional term added to the system dynamics now represent the effect of system faults. The model of the actuator power loss failure can be represented as[17]

$$u_f = E_f u \tag{15}$$

$E_f \in \mathrm{R}^{mxn}$ is the actuator fault matrix with the following diagonal structure

$$E_f = \begin{bmatrix} \varepsilon_{f1} & 0 & .... & 0 \\ 0 & \varepsilon_{f2} & .... & 0 \\ .... & .... & .... & 0 \\ 0 & 0 & 0 & \varepsilon_{fn} \end{bmatrix} \tag{16}$$

where

$\varepsilon_{fi} = 0$ represents power loss

$0 < \varepsilon_{fi} < 1$ represents fading power

$\varepsilon_{fi} = 1$ represents healthy actuator

$i = 1, 2, ..., n$

Properties

The faulty dynamics defined in Eq. (15) have the following properties.

- The matrix E_f is a diagonal matrix that is positive definite. This fact can be verified by observing the limits of ε_{fi}.
- Such matrix is nonsingular; therefore all the eigen values are non-zero.
- It is real symmetric; therefore all the eigen values are real numbers.
- The eigen values of such matrix can be given as :

  $E_f = diag\left(\varepsilon_{f1}.....\varepsilon_{fn}\right)$

  $\Rightarrow \varepsilon_{f1}....\varepsilon_{fn}$ are eigen values of E_f

Thus, the dynamics of the RLV Eq. (13) become

$$\ddot{x} = \frac{d}{dt}A(.) + BC + \left[\frac{d}{dt}B(.) + BD\right]y + RE_f u + f_f \tag{17}$$

Define error dynamics as

$$e = x - x^* \text{ and } s = \dot{e} + k_0 e \tag{18}$$

where $k_0 > 0$ is a design constant. The control gain is represented as follows

$$R = BE = R_0 + \Delta R$$

Error dynamics of Eq. (17) can be simplified with the error function defined as in Eq. (18) and represented as:

$$\dot{s} = f_0 + \Delta f + R_0 E_f u \tag{19}$$

where

$$\begin{aligned} f_0 &= BC + BD\dot{y} - \ddot{x}^* + k_0\dot{e} - \text{Known, Time variant} \\ \Delta f &= \frac{d}{dt}A(.) + \frac{d}{dt}B(.)y + \Delta R E_f u \pm f_f - \text{Unknown, Timevairant} \\ R_0 &- \text{Known Part of control gain} \\ \Delta R &- \text{Unknown Part of control gain} \end{aligned} \tag{20}$$

Note for the sake of simplicity, the arguments of the functions were omitted, even though this does not affect the clarity. Also a part of control gain R_0 is available if not the total control gain RE_f. The framework for a control to deal with this type of failures is illustrated in Figure 10.

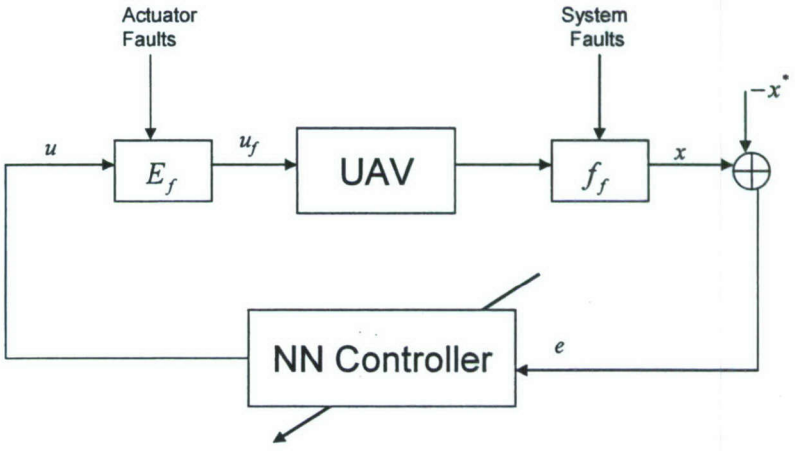

Figure 10 - Controller framework for fault tolerance

Assumptions:

For the system to admit a feasible solution under faulty condition, we need to assume that there exists a positive constant $c_0 > 0$ such that $\|\Delta R\| + c_0 \le \|R\|$

Properties:

1) Matrix E is known from the literature as being invertible. As for matrix B, the control surfaces of the UAV are designed to control angular rate along each axis of the aircraft independently; therefore, the matrix B is invertible for all cases. Numerical studies for the aerodynamic model also show that B is always invertible.

2) $E_f^{-1} = E_f^{-T} > 0$

3) If R_0 is full row rank, then there exist constants c_{min} and c_{max} such that

$$c_{\min}\|s\|^2 \le s^T R_0 E_f R_0^T s \le c_{\max}\|s\|^2$$

where $c_{max} \geq c_{min} > 0$ denotes the maximum and the minimum eigen values of $R_0 E_f R_0^T$ respectively. This proposition is valid since the matrix is symmetric and positive-definite. This can be justified by noting that E_f is a diagonal matrix and $R_0 = BE$ is invertible as explained above. Also observing the properties of E_f defined in the previous section, the matrix $R_0 E_f R_0^T$ has positive, real eigen values.

Now we proceed to design an adaptive control algorithm for the above described highly coupled, nonlinear, uncertain, faulty complex system.

C.3. Neuro-adaptive Fault-tolerant Control Design

The major challenge in control design for the above described system is the nonlinear and uncertain nature of ΔR and Δf. The basis for most stable adaptive controllers has been to reorganize Δf as a linear combination. However, this method is not suitable for complex systems such as aircrafts since it involves complicated design procedures and heavy computations. Another approach is to estimate Δf via multilayer NNs and train these networks via gradient algorithms. Recognizing the potential instability associated with these algorithms, several researchers have proposed NN control schemes using on-line and stable training mechanism based on Lyapunov stability theory. We further extend these works in an innovative path.

We "reconstruct" Δf via the first NN unit as

$$f_{NN} = f_0 + W_1^T \psi_1$$

Where

f_0 the available part of f

$W_1 \in R^{mxm}$ the optimal weight of the NN

$\psi_1 \in R^m$ the base function of NN whose selection typically include linear function, sigmoid function, hyperbolic tangent function, radial basis function, etc.

Let the discrepancy between f and f_{NN} be denoted by:

$$\varepsilon = f - f_{NN} \tag{21}$$

where ε is the reconstruction error. With the support of the approximate theory of multilayer neural networks, such an error can be made arbitrarily small provided that certain conditions (e.g., sufficiently large numbers of neurons, sufficient smoothness of f etc.) are satisfied. This has been the basis for many NN based control laws. In reality, however, it should be noted that one can only use a network with a finite number of neurons and that the nonlinear function being reconstructed is not smooth enough. Thus, during system operations, the reconstruction error sometimes is bounded by a constant, but at other times it may not necessarily be confined to that number. For this reason, simply assuming that $||\varepsilon||$ is uniformly bounded by a constant does not warrant the success of the control scheme, as seen in Figure 11[18].

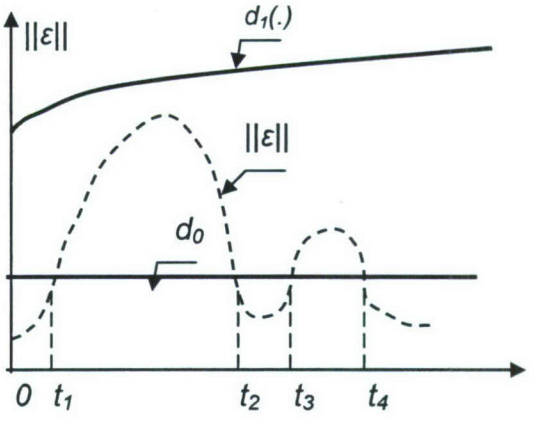

Figure 11 - The possible profile of NN reconstruction error

For executing the idea, in our development, we remodel reconstruction error as follows

$$\varepsilon = c\varepsilon_1 + (1-c)\varepsilon_2$$

$$\text{with } c = \begin{cases} 1 & \text{if the NN works satisfactorily} \\ 0 & \text{if the NN fails to work well} \end{cases}$$

To make the problem solvable, we make the assumption that

$$\| \varepsilon_1 \| \leq d_0 < \infty, \quad \text{and } \| \varepsilon_2 \| \trianglelefteq \| f - f_0 - W_1^T \psi_1 \| \trianglelefteq d_1(.).$$

The point to be made is that d_0 and $d_1(.)$ are still unavailable and should not be included in the control scheme directly. Another major challenge due to the fact that we do not know when the NN behaves well. Sanner and Slotine[19] proposed a method of partitioning the state space into A_d and A_d^c and assumed that the NN works satisfactorily within A_d. Here we take a different method to address this issue. Namely, we incorporate two NN units in the control scheme, with the first NN unit compensating the lumped nonlinearities/uncertainties and the second NN unit attenuating the effects due to the NN reconstruction error and the other resulting uncertainties. The overall control scheme is given by

$$u = R_0^T \left(-k_0 s - \hat{f}_{NN} - u_{ca} \right) \tag{22}$$

The estimate neural network of the uncertain part Δf is:

$$\hat{f}_{NN} = f_0 + \hat{W}_1^T \psi_1 \tag{23}$$

The terms used in the controller and estimation of the first neural network are:

u_{ca} = a compensating signal to be specified

$k_0 > 0$ = a constant chosen by the designer

$\hat{W}_1$ = is the estimate of the ideal weight values

Before defining the signal u_{ca} the following signals and scenarios are to be considered. It is interesting to observe that the control algorithm remains unaffected even though the control gain

is considerably affected by the actuator failures. This is one of the features of the neuro-adaptive controller. It adapts to the changes in the uncertainty without necessitating the changes in the control algorithm. With the control of the above scheme, the original system Eq. (19) becomes

$$\dot{s} = -k_0 R_0 E_f R_0^T s + \tilde{W}_1^T \psi_1 - R_0 E_f R_0^T u_{ca} + \eta \tag{24}$$

where $\tilde{W}_I = W_I - \hat{W}_I$ is weight estimation error and

$$\eta = \varepsilon + \left(I - R_0 E_f R_0^T\right)\left(f_0 + \hat{W}_1^T \psi_1\right) \tag{25}$$

is the resultant uncertainty to be attenuated by the second NN unit. Expressing η in a similar fashion as done earlier, we have, $\|\eta\| \le \gamma_a$

$$\gamma_a = \sum_{i=1}^{N_1+3} \omega_i Y_i \tag{26}$$

where N_I is an integer. The weights and scalar function are defined as:

$$\omega_{N_1+1} = d_0, \omega_{N_1+2} = \|W_I\|, \omega_{N_1+3} = \sup_{s \in R_c \subset R^m} \|I - R_0 E_f R_0^T\|$$

$$\text{and} \quad Y_{N_1+1} = 1, Y_{N_1+2} = \|\psi_I\|, Y_{N_1+3} = \|\hat{W}_I \psi_I\|$$

γ_a is estimated as

$$\hat{\gamma}_a = \sum_{i=1}^{N_a} \hat{\omega}_i \psi_{II}(Y_i) = \hat{\omega}^T \psi_{II}(Y) \tag{27}$$

where $N_a = N_1 + 3$, $\hat{\omega}_i$ denote the estimate weights and $\psi_{II_i}(\cdot)$ are some basis functions satisfying

$$\psi_{II_i}(Y_i) \ge Y_i \tag{28}$$

The compensating signal can now be defined as:

$$u_{ca} = \frac{\sum_{i=1}^{N_a} \psi_{II_i} \hat{\omega}^T \psi_{II}(Y)}{\sum_{i=1}^{N} \psi_{II_i} \|s\| + v} s \tag{29}$$

C.3.1. Stability Analysis

For all control systems, and for adaptive control systems, stability is the primary requirement. In this section we use the Lyapunov's stability theory to prove that the proposed new adaptive scheme in the above section is able to achieve the control objective. We choose a Lyapunov candidate function

$$V = V_1 + V_2 + V_3 \tag{30}$$

with

$$\begin{aligned} V_1 &= \frac{1}{2} s^T s, \quad V_2 = \frac{1}{2g_I} tr(\tilde{W}_1^T \tilde{W}_1), \\ V_3 &= \frac{1}{2g_{II} c_{\min}} (\omega - c_{\min}\hat{\omega})^T (\omega - c_{\min}\hat{\omega}) \end{aligned} \tag{31}$$

where $g_I > 0$ and $g_{II} > 0$ are free design parameters affecting weight learning rate and control performance, $c_{\min} > 0$ is the minimum eigen value of RE_fR^T. Its derivative along the vector field is

$$\begin{aligned} \dot{V}_a &= -k_0 s^T \left(R_0 E_f R_0^T\right) s + s^T \tilde{W}_1^T \psi_1 \quad + s^T \eta - s^T R_0 E_f R_0^T u_{ca} + \dot{V}_2 + \dot{V}_3 \\ &\le -k_0 c_{\min} \|s\|^2 + Q \; + tr\left(\tilde{W}_1^T \left(\psi_1 s^T - g_1^{-1} \dot{\hat{W}}\right)_1\right) \end{aligned}$$

with

$$Q = s^T \eta - s^T R_0 E_f R_0^T u_{ca} - \frac{1}{g_{II}} (\omega - c_{\min}\hat{\omega})^T \dot{\hat{\omega}} \tag{32}$$

Before presenting the weight tuning algorithms, let us focus on Q. With u_{ca} as in Eq. (30) and the upper norm bound on η as in Eq. (25), we have

$$\begin{aligned} Q &\le \|s\| \omega^T Y - \frac{c_{\min} \sum_{i=1}^{N} \psi_{II_i} \|s\|^2 \hat{\omega}^T \psi_{II}}{\sum_{i=1}^{N} \psi_{II_i} \|s\| + v} - \frac{1}{g_{II}} (\omega - c_{\min}\hat{\omega})^T \dot{\hat{\omega}} \\ &= (\omega - c_{\min}\hat{\omega})^T \left[\frac{\sum_{i=1}^{N} \psi_{II_i} \|s\|^2 \psi_{II}}{\sum_{i=1}^{N} \psi_{II_i} \|s\| + v} - \frac{1}{g_{II}} \dot{\hat{\omega}} \right] + v\omega_m \end{aligned} \tag{33}$$

where $\omega_m = \max(\omega_i)$. Note that in deriving the above equation, we have used the facts that

$$\omega^T Y \le \omega^T \psi_{II} \le \omega_m \sum_{i=1}^{N} \psi_{II_i} \quad \text{and} \quad \frac{\sum_{i=1}^{N_a} \psi_{II_i} \|s\|}{\sum_{i=1}^{N_a} \psi_{II_i} \|s\| + v} \le 1, \quad \forall v > 0$$

Combining Eq. (33) and Eq. (34), we come up with the following weight tuning algorithms:

$$\dot{\hat{W}}_I = -\sigma_I \hat{W}_I + g_I \psi_I s^T$$
$$\dot{\hat{\omega}} = -\sigma_{II} \hat{\omega} + g_{II} \frac{\sum_{i=1}^{N_a} \psi_{II_i} \|s\|^2 \psi_{II}}{\sum_{i=1}^{N_a} \psi_{II_i} \|s\| + v} \tag{34}$$

Consequently,

$$\dot{V} \leq -c_{\min} k_0 \| s \|^2 + \frac{\sigma_I}{g_I} tr(\tilde{W}_I^T \hat{W}_I) + \frac{\sigma_{II}}{g_{II}} (\omega - c_{\min} \hat{\omega})^T \hat{\omega} + v\omega_m \tag{35}$$

Completing the square we can further rewrite Eq. (36) as:

$$\dot{V} \leq -c_{\min} k_0 \| s \|^2 - \frac{\sigma_I}{2g_I} tr(\tilde{W}_I^T \tilde{W}_I) - \frac{\sigma_{II}}{2g_{II} c_{\min}} (\omega - c_{\min} \hat{\omega})^T (\omega - c_{\min} \hat{\omega}) + \delta = -\lambda_1 V_1 - \lambda_2 V_2 - \lambda_3 V_3 + \delta \tag{36}$$

where

$$\delta = v\omega_m + \frac{\sigma_I}{2g_I} tr(W_I^T W_I) + \frac{\sigma_{II}}{2g_{II}} \omega^T \omega \tag{37}$$

$$\text{and } \lambda_1 = 2c_{\min} k_0, \quad \lambda_2 = \sigma_I, \quad \lambda_3 = \sigma_{II} \tag{38}$$

are constants independent of s. Note that Eq. (37) implies that $\|s\|$, $\hat{W}_I$ and $\hat{\omega}$ are bounded. Furthermore, from Eq. (37), we have

$$\dot{V} \leq -k_0 c_{\min} \|s\|^2 + \delta \tag{39}$$

It is seen that $\dot{V}$ is negative as long as

$$\|s\| \geq \sqrt{\left(\frac{\delta}{k_0 c_{\min}} \right)} \tag{40}$$

Therefore, s is confined in the region $\Omega = \left\{ s \,|\, \|s\| \le \left(\frac{\delta}{k_0 c_{\min}} \right)^{1/2} \right\}$. From previous lemma, we establish that the control error is bounded.

C.3.2. Control Strategy with Alternate Gain

An alternate control gain can also be used to achieve the above performance. This alternate gain enhances the performance of the control but the inverse is tedious to compute. The neuro-adaptive control for the system described as in Eq. (19) is given as:

$$u = R_0^{-1}\left(-k_0 s - \hat{f}_{NN} - u_{ca}\right) \tag{41}$$

where all the terms are as defined in the previous section.

Properties

1) The matrix E_f is a diagonal matrix that is positive definite. This fact can be verified by observing the range of ε_{fi}.

2) Such matrix is nonsingular; therefore all the eigenvalues are non-zero.

3) It is real symmetric; therefore all the eigenvalues are real numbers. The eigenvalues of such matrix can be given as :

$$\begin{aligned} &E_f = diag\left(\varepsilon_{f1}.....\varepsilon_{fn}\right) \\ &\Rightarrow \varepsilon_{f1}....\varepsilon_{fn} \text{ are eigen values of } E_f \end{aligned} \tag{42}$$

4) Matrix E is known from the literature as being invertible. As for matrix B, the control surfaces of the reusable launch vehicle are designed to control angular rate along each axis of the aircraft independently; therefore, the matrix B is invertible for all cases. Numerical studies for the aerodynamic model also show that B is always invertible.

5) f R_0 is full row rank, then there exist constants c_{min} and c_{max} such that

$$c_{\min}\|s\|^2 \le s^T \left\| R_0 E_f R_0^{-1} \right\| s \le c_{\max}\|s\|^2 \tag{43}$$

where $c_{\max} \ge c_{\min} > 0$ are the eigenvalues of the matrix $R_0 E_f R_0^{-1}$.

$$c_{\min} = \min\left(eig\left(E_f\right)\right) = \varepsilon_{f\min} > 0 \qquad \text{and} \quad c_{\max} = \max\left(eig\left(E_f\right)\right) = \varepsilon_{f\max} > 0 \tag{44}$$

With the control of the above scheme, the original system Eq. (19) becomes

$$\dot{s} = -k_0 R_0 E_f R_0^{-1} s + \tilde{W}_1^T \psi_1 - R_0 E_f R_0^{-1} u_{ca} + \eta$$

where $\tilde{W}_I = W_I - \hat{W}_I$ is weight estimation error and

$$\eta = \varepsilon + \left(I - R_0 E_f R_0^{-1}\right)\left(f_0 + \hat{W}_1^T \psi_1\right) \tag{45}$$

is the resultant uncertainty to be attenuated by the second NN unit. Expressing η in a similar fashion as done earlier, we have, $\|\eta\| \le \gamma_a$

$$\gamma_a = \sum_{i=1}^{N_1+2} w_i Y_i \tag{46}$$

where N_I is an integer. The weights and scalar function are defined as:

$$w_{N_1+1} = d_0,\ w_{N_1+2} = \|W_I\| \quad \text{and} \quad Y_{N_1+1} = 1,\ Y_{N_1+2} = \|\psi_I\|$$

γ_a is estimated as

$$\hat{\gamma}_a = \sum_{i=1}^{N_a} \hat{w}_i \psi_{II}(Y_i) = \hat{w}^T \psi_{II}(Y) \tag{47}$$

where $N_a = N_1 + 2$, $\hat{\omega}_i$ denote the estimate weights and $\psi_{II_i}(.)$ are some basis functions satisfying

$$\psi_{II_i}(Y_i) \ge Y_i \tag{48}$$

The compensating signal can now be defined as:

$$u_{ca} = \frac{\sum_{i=1}^{N_a} \psi_{II_i} \hat{w}^T \psi_{II}(Y)}{\sum_{i=1}^{N} \psi_{II_i} \|s\| + v} s \tag{49}$$

C.3.3. Stability Analysis of the Control Strategy with Alternate Gain

We choose a Lyapunov candidate function same as described in the previous section. Its derivative along the vector field is

$$\begin{aligned} \dot{V}_a &= -k_0 s^T R_0 E_f R_0^{-1} s + s^T \tilde{W}_1^T \psi_1 + s^T \eta - s^T R_0 E_f R_0^{-1} u_{ca} + \dot{V}_2 + \dot{V}_3 \\ &\le -k_0 c_{\min} \|s\|^2 + Q + tr\left(\tilde{W}_1^T \left(\psi_1 s^T - g_1^{-1} \dot{\hat{W}}\right)_I\right) \end{aligned}$$

with

$$Q = s^T \eta - s^T R_0 E_f R_0^{-1} u_{ca} - \frac{1}{g_{II}} \left(w - c_{\min} \hat{w}\right)^T \dot{\hat{w}} \tag{50}$$

Before presenting the weight tuning algorithms, let us focus on Q. With u_{ca} as in Eq. (49) and the upper norm bound on η as in Eq. (45), we have

$$\begin{aligned} Q &\le \|s\| w^T Y - \frac{\sum_{i=1}^{N} \psi_{II_i} \|s\|^2 \hat{w}^T \psi_{II}}{\sum_{i=1}^{N} \psi_{II_i} \|s\| + v} - \frac{1}{g_{II}} \left(w - c_{\min} \hat{w}\right)^T \dot{\hat{w}} \\ &= \left(w - c_{\min} \hat{w}\right)^T \left[\frac{\sum_{i=1}^{N} \psi_{II_i} \|s\|^2 \psi_{II}}{\sum_{i=1}^{N} \psi_{II_i} \|s\| + v} - \frac{1}{g_{II}} \dot{\hat{w}} \right] + v w_m \end{aligned} \tag{51}$$

Note the expression for the signal Q is the same as Eq. (34). Thus, the rest of the stability analysis follows the previous section and we can prove that the control error is bounded in the region described as in Eq. (40).

The control strategy change does not affect the performance of the controller in any way although the gain described in section A is easier to compute than the gain of control strategy described in the above section, but the latter method gives a better tracking precision.

C.4. Simulation Results

In this section, we present a series of simulations to illustrate the effectiveness of the proposed neuro-adaptive fault-tolerant control in tracking a desired angle of attack α, sideslip β and body-axis roll Φ of the UAV.

Table 2: Numerical Values Used for Simulation

Parameter	Symbol	Units	Value
Wing Area	S	m^2	391.2
Thrust	T	Lb	27,000
Mean Aerodynamic Chord	$\bar{c}$	Ft	11.32
Roll Inertia	I_x	$kg.m^2$	1,997,922
Pitch Inertia	I_y	$kg.m^2$	276,629,966.8
Yaw Inertia	I_z	$kg.m^2$	28,383,800
UAV Mass	M	Kg	103,756
Wing Span	B	M	29.2
UAV Velocity	V	Mach	0-15

The control strategy explained in earlier is utilized. Matlab is used for the simulation. The coefficients similar to the model X-33 are used. The simulation models include all non-linearity in the equations of motion, and the values of the parameters and coefficients are given as in Table 2[15, 16, 20]. The payload mass is considered to be zero in the reentry phase and the mass of fuel is considered to be exponentially decreasing non-zero function with respect to time as $m_f = m_{f(\text{int.})} * e^{-t}, t$ – Time in seconds .

We chose the basis functions for the first NN unit as:

$$\psi_I(c_{1i}, X, \gamma) = \frac{1 - e^{-\lambda(\|X\| - c_{1i})^2}}{1 + e^{-\lambda(\|X\| - c_{1i})^2}},$$

$$c_{1i} = 0.2, 0.4, \ldots, \|X\| = \begin{bmatrix} \alpha \\ \beta \\ \phi \end{bmatrix},$$

$$\lambda = 0.5.$$

The basis functions for the second NN unit are selected as :

$$\psi_{II}(Y) = Y, Y = \left[\|X\| \quad \|\dot{X}\| \quad u \quad . \quad . \quad 1 \quad \psi_I\right], \|X\| = \begin{bmatrix} x \\ y \\ z \end{bmatrix}.$$

Fifteen NN basis functions were used for each of the NN units: $\psi \in R^j$, $j = 15$. All the weights are initialized at zero in the simulation. The command values of α, β and Φ are applied to the UAV are $\alpha^* = 0.8 + 0.1\sin\frac{t}{6}$, $\beta^* = 0.1 + 0.2e^{-t}$, $\phi^* = 0.8 + 0.01\cos t$.

The system faults for the numerical simulation are chosen to occur after 15 seconds and continue to appear till the end of the simulations. The faults represented in Eq. (14) with $\alpha = 0.5$ were chosen.

The actuator faults occur after 30 seconds and also continue to appear all along till the end of simulations. These faults are modeled based on Eq. (16) with ε_{fi} chosen as

$$\varepsilon_{fi} = \begin{cases} 1, & t \le 30 \\ 1 - 1/i * \left|\sin(t - i)\right|, & t > 30 \end{cases}, i = 1 \ldots . n$$

Figure 12 – Figure 18 shows the system response when the actuator power and sensors fail. Each figure has the actual and desired paths, the tracking error, and the action of the control, profile of faults and estimated weights for the first and second NN. It can be seen that the tracking is achieved within a small error. Note that the first NN weights remain unaffected by the fault occurrence.

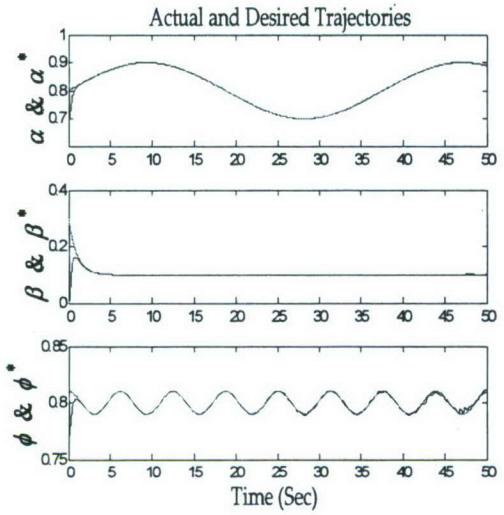

Figure 12 - Actual and desired trajectories

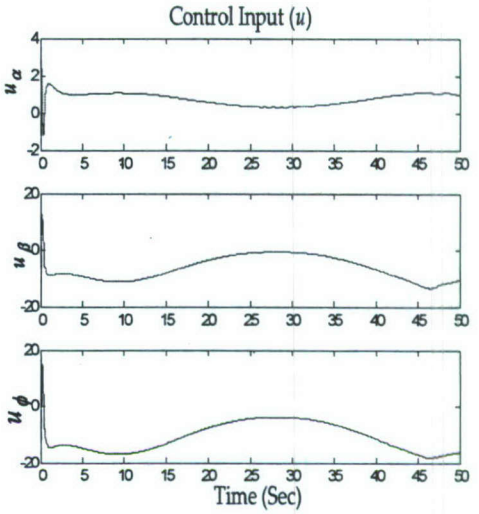

Figure 13 - Control inputs

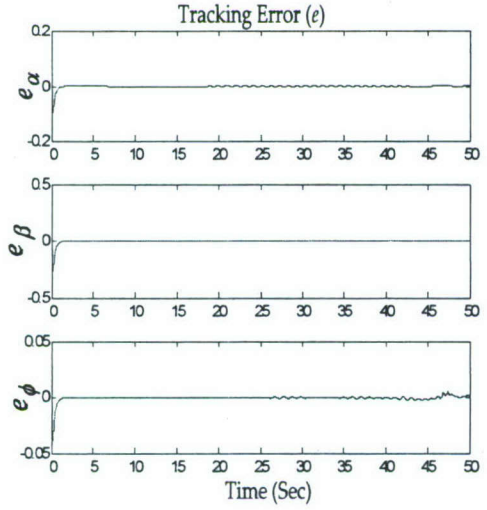

Figure 14 - Trajectory Errors

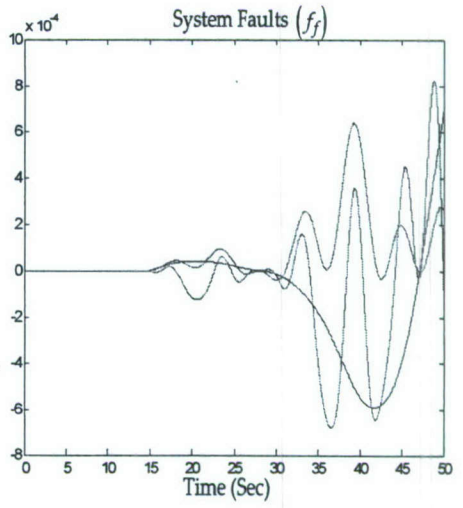

Figure 15- System Faults Profile

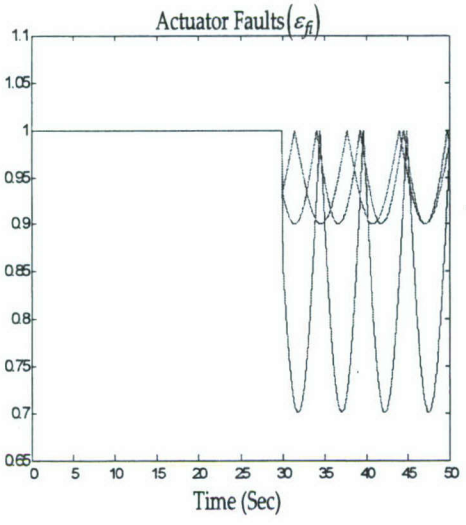

Figure 16 - Actuator faults profile

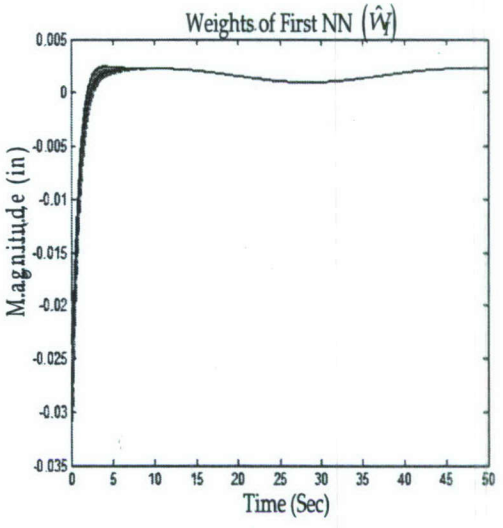

Figure 17 - Weights profile of first NN

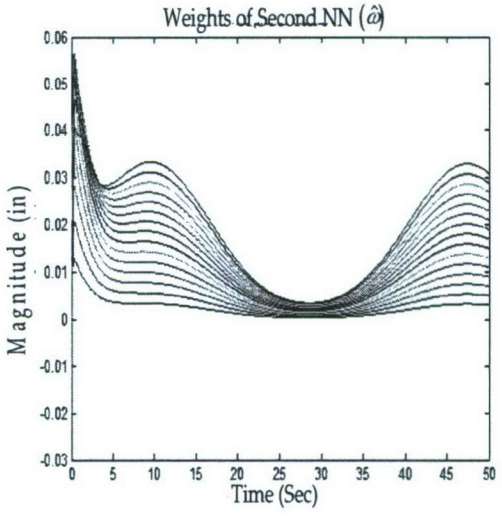

Figure 18 - Weights profile of funneling NN

The effect of number of neurons used for the neural networks plays a vital role in the effectiveness of the controller. It can be observed from the results presented above that the system reaches stability when 15 neurons were used. But the tracking precision can be improved by increasing the number of neurons in the NN. Figure 19 – Figure 23 shows the system responses when 25 neurons were used to represent a layer under system and actuator failures. It can be observed that even though the tracking precision is improved by a small amount, the controller exhibits chattering effect, which is a negative performance criterion for any control strategy. This trade-off is to be decided by the designer based on the nature of the plant. Design parameters like g_I and g_{II} aid in reducing this chattering but do not completely avoid.

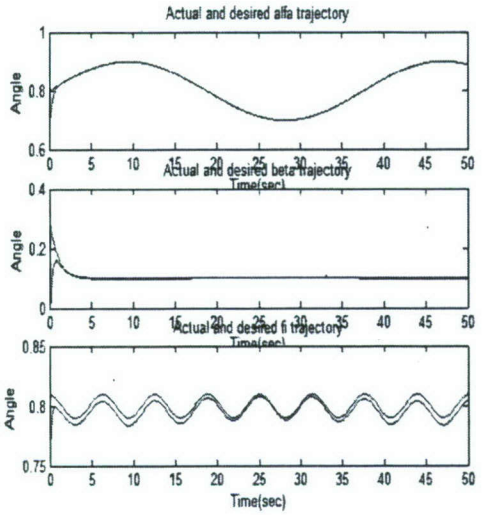

Figure 19 - Actual and desired trajectories

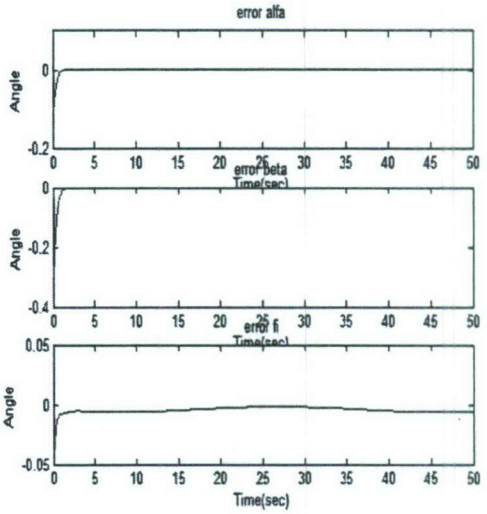

Figure 20 - Trajectory errors

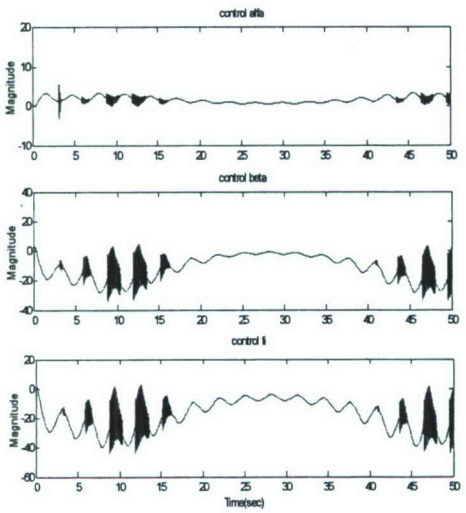

Figure 21- Controls inputs

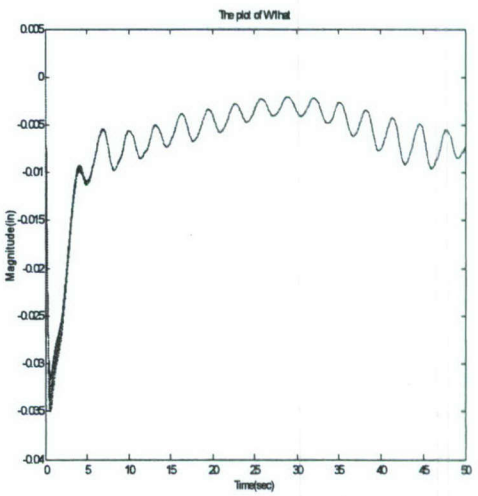

Figure 22 - Weights profile of first NN

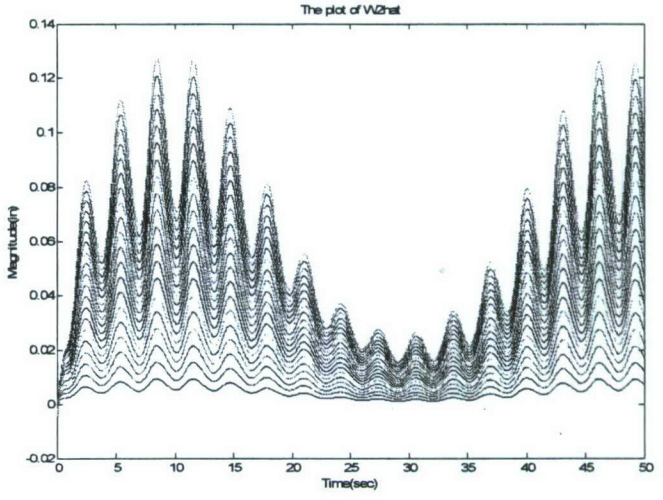

Figure 23 - Weights profile of the funneling NN

Project Publications

1. Bin Li, Zhao Sun, X. H. Liao, Liguo Weng, and Y. D. Song, "3D Robust Formation Control of Multi-UAVs," *6th International Conference on Cooperative Control and Optimization*, February, 2006.
2. S. Kanury and Y. D. Song,"Flight Management of Multiple Aerial Vehicles Using Genetic Algorithms," *2006 IEEE Southeast Symposium on Systems Theory*, Cookeville, TN,pp.33-37,March, 2006.
3. X. H. Liao, Zhao Sun, Tao Dong, Bin Li, and Y. D. Song, "GA-based Disturbance Attenuation in Flight Control Systems," *2006 IEEE Southeast Symposium on Systems Theory*, Cookville, TN, pp.519-523, March, 2006.
4. Bin Li, X. H. Liao, Zhao Sun, Wenchuan Cai and Y. D. Song, "Robust Formation Following Control of Multi-flight Vehicles," *2006 IEEE Southeast Symposium on System Theory*, Cookeville, TN,pp.294-298, March, 2006.
5. X. H. Liao, Zhao Sun and Y. D. Song, "Chattering-free Variable Structure Control with Application to Flight Vehicles," *2006 IEEE Southeast Symposium on Systems Theory*, Cookeville, TN, pp. 406-410, March, 2006.
6. Liguo Weng, Wenchuan Cai, M. J. Zhang, X. H. Liao and David Song, "*Neural-Memory Based Control of Micro Air Vehicles (MAVs) with Flapping Wings*," *4th International Symposium on Neural Networks*, Nanjing, China, June 3-7, 2007.
7. Yao Li, Zhao Sun, Ran Zhang, Liguo Weng, and David Y. Song, "Close Formation Flight Control of Multi-UAVs via Fuzzy Logic Technique," Advanced Fuzzy Logic Technologies in Industrial Applications ,chp. 16, 2006.
8. Yaohang Li , T. Dong, M. Bikdash, Y. Song, "Path Planning for Unmanned Vehicles using Ant Colony Optimization on a Dynamic Voronoi Diagram," International Conference on Artificial Intelligence, Las Vegas NV, 2006.

9. Liguo Weng, Wenchuan Cai, Ran Zhang, David Song, "Human Memory/Learning Inspired Approach for Flapping-wing Motion Control of Micro Air Vehicles (MAVs)," *International Journal of Modelling, Identification and Control (under review)*, 29 June - 2 July 2008, Shanghai, China.

Presentations

- *Cooperative Control and Optimization 2007,* February *2007,Florida*
- *IEEE 38th Southeastern Symposium on Systems Theory (SSST 06). March 2006,Tennessee*
- *American Institute of aeronautics and astronautics (*AIAA) Space 2007 Conference and Exposition, *Sep. 2007, Long Beach, CA*
- *AIAA Guidance, Navigation and Control Conference and Exhibit 2007, Sep. 07,*

Appendix I -Nomenclature

b	=	UAV wingspan
$\bar{c}$	=	Wing Mean Reference Chord
m	=	UAV Variable mass
p, q, r	=	Roll, Pitch and Yaw rates/body fixed frame
$\bar{q}$	=	Free-Stream dynamic pressure
S	=	Wing Reference Area
T	=	Thrust
V	=	UAV variable velocity
F	=	Aerodynamic Force about the body frame
L, M, N	=	Aerodynamic Rolling, Pitching and Yawing Moments
α, β	=	Angle of Attack and Side-slip
ϕ, θ, ψ	=	Roll, Pitch and Yaw Euler angles
$\delta_e, \delta_a, \delta_r$	=	Elevator, Aileron and Rudder deflections
ρ	=	Air Density
C	=	Aerodynamic Force Coefficient

References

[1]Zhou, D. H., & Frank, P. M. , "Fault diagnostics and fault tolerant control", *IEEE Transactions on Aerospace & Electronic Systems*, Vol. 34, No. 2, 1998, pp. 420–427

[2]Willsky, A. S., "A survey of design methods for failure detection in dynamic systems", *Automatica,* Vol. 12,1976, pp. 601–611

[3]Siljak, D. D., "Reliable control using multiple control systems" ,*International Journal of Control,* Vol. 31, No. 2, 1980, pp. 303–329

[4]Yang, G. H., Zhang, S. Y., Lam, J., & Wang, J. ,"Reliable control using redundant controllers", *IEEE Transactions on Automatic Control,* Vol. 43, No. 11, 1998, pp. 1588–1593

[5]Rauch, H. E., "Autonomous Control Reconfiguration," *IEEE Control Systems,* 1995, pp. 37-48

[6]Kwong, W. A., K. M. Passino, E.G. Laukonen, and S. Yurkovich, "Expert Supervision of Fuzzy Learning Systems for Fault Tolerant Aircraft Control," *Proceedings of the IEEE*, Vol. 83, No. 3, 1995, pp. 342-351

[7]Layne, J. R. and K. M. Passino, "Fuzzy Model Reference Learning Control for Cargo Ship Steering," *IEEE Control Systems Magazine*, 1993.

[8]Moudgal, V., W. A. Kwong, K. M. Passino, and S. Yurkovich, "Fuzzy Learning Control for a Flexible-Link Robot," *IEEE Trans. on Fuzzy Systems,* Vol. 3, No. 2, 1995

[9]Passino, K. M., "Intelligent Control for Autonomous Systems," *IEEE Spectrum,* 1995

[10]Rauch H. E. "Intelligent Fault Diagnosis and Control Reconfiguration" *IEEE International Symposium on Intelligent Control,* 1994

[11]Polycarpou M., Zhang X., Xu R., Yang Y. Kwan C., "A Neural Network Based Approach to Adaptive Fault Tolerant Flight Control" *Proceedings of IEEE International Symposium on Intelligent Control*, 2004

[12]Chen J., Patton R. J., Chen Z., "An LMI Approach to Fault-tolerant Control of Uncertain Systems" *Proceedings of the 19: 8 IEEE ISIC/CIRA/ISAS Joint conference* , 1998, pp. 14-17

[13]Boskovik J. D., Li S., and Mehra R. K., "A Decentralized Fault-Tolerant Scheme for Flight Control Applications" *Proceedings of the American Control Conference* , 2000

[14]Q.Wu, M. Saif, "Neural Adaptive Observer Based Fault Detection and Identification for Satellite Attitude Control Systems", *American Control Conference*, 2005, pp. 1054-1059

[15]Brian, S and Frank L. L, *Aircraft control and simulation*, John Wiley & Sons, 1992

[16]Morelli, E. A., "Global Nonlinear Parametric Modeling with Application to F-16 Aerodynamics," *Proceedings of the 1998 American Control Conference, IEEE Publications,* pp. 997-1001, 1998

[17]Jie Baoa, Wen Z. Zhanga and Peter L. Leeb "Decentralized fault-tolerant control system design for unstable processes", *Chemical Engineering Science* Vol.58 , 2003, pp. 5045 – 5054

[18]F. C. Chen and C. C. Liu, "Adaptively Controlling Nonlinear Contiguous-Time Systems Using Multilayer Neural Networks," *IEEE Trans. on Auto. Control*, Vol. 39, No. 6, 1994, pp. 1306-1310

[19]Karakasoglu, S. I. Sudharsanan and M. K. Sundareshan, "Identification and Decentralized Adaptive Control Using Dynamical Neural Networks with Application to Robotic Manipulators," *IEEE Trans. on Neural Networks*, Vol. 4, No. 6, 1993, pp. 919-930

[20]Taeyoung, Lee and Youdan Kim, "Nonlinear Adaptive Flight Control Using Backstepping and Neural Networks Controller", *AIAA*, Vol. 24. No. 4 ,1995

REPORT DOCUMENTATION PAGE

Form Approved
OMB No. 0704-0188

1. REPORT DATE *(DD-MM-YYYY)*	2. REPORT TYPE	3. DATES COVERED *(From - To)*
29-02-2008	Final	01/03/2003-30/06/2007

4. TITLE AND SUBTITLE
Fault-tolernat and Reconfigurable Control of Unmanned Air Vehicles (UAVs)

5a. CONTRACT NUMBER

5b. GRANT NUMBER
N00014-03-1-0462

5c. PROGRAM ELEMENT NUMBER

6. AUTHOR(S)
Song, Yong D.

5d. PROJECT NUMBER

5e. TASK NUMBER

5f. WORK UNIT NUMBER

7. PERFORMING ORGANIZATION NAME(S) AND ADDRESS(ES)
North Carolina A&T State University
1601 E. Market Street
Greensboro, NC 27411

8. PERFORMING ORGANIZATION REPORT NUMBER
210022

9. SPONSORING/MONITORING AGENCY NAME(S) AND ADDRESS(ES)
OFFICE OF NAVAL RESEARCH
875 NORTH RANDOLPH STREET
ARLINGTON, VA 22203-1995

10. SPONSOR/MONITOR'S ACRONYM(S)

11. SPONSORING/MONITORING AGENCY REPORT NUMBER

12. DISTRIBUTION AVAILABILITY STATEMENT
Approved for Public Release; Distribution is Unlimited.

13. SUPPLEMENTARY NOTES

14. ABSTRACT
Unmanned aerial vehicles (UAVs) are critical components of the future naval forces. UAV control and monitoring with autonomous operation will become an absolute necessity and adaptive cooperation of vehicles is the only practical alternative. The objective of this project is to develop and evaluate new methodologies for cooperative (formation) control of multiple unmanned air vehicles. The goal is to have multiple UAVs working together as a group. Instead of separately assigning distinct tasks to each vehicle, the operator would assign tasks to the UAV group, which then determines the best way to accomplish each task, freeing the operator to maintain surveillance over the entire operation. In this project we investigated Path Tracking and obstacle avoidance of UAVs using fuzzy logic method. Algorithms for close formation control of multi-UAVs are developed and simulated. We also investigated fault-tolerant control of single UAVs by neuro-adaptive method. Detailed description of this method is provided in this document. The project has supported 5 graduate students with 9 technical papers published.

15. SUBJECT TERMS

16. SECURITY CLASSIFICATION OF:			17. LIMITATION OF ABSTRACT	18. NUMBER OF PAGES	19a. NAME OF RESPONSIBLE PERSON
a. REPORT	b. ABSTRACT	c. THIS PAGE		30	DR. YONG D. SONG
					19b. TELEPONE NUMBER *(Include area code)* 336-334-7760